Pall Corporation: Changes in membrane filter capture efficiency due to folding

Academic Contributors:
L.J. Cummings*(linda.cummings@njit.edu); D. Bramer (bramerda@msu.edu);
J. Brimlow (jbrimlow@gmail.com); R.J. Dyson (r.j.dyson@bham.ac.uk);
C. Exley (cde4@sfu.ca); E. Fagerstrom (emilyrf@buffalo.edu);
A. Korn (pmxak@nottingham.ac.uk); S. Li (sisili@seas.harvard.edu);
L. McCormick (lmccorm@g.clemson.edu); A. Peace (angela.peace@asu.edu);
M. Takeuchi (melody.takeuchi@gmail.com); B. Tilley (tilley@wpi.edu);
M. Zemsky (MCZemsky@wpi.edu).
Industrial Participants:
Mark Hurwitz, Matt Lucey, Yueyang Shen

September 17, 2013

Abstract

Pall Corporation makes very fine porous filter media out of PTFE with ratings in the range of nanometers. They are interested in predicting the changes that may occur in the ability of the membrane to capture particles of various sizes when the filter is pleated to make a filter cartridge. This report examines the effects of the folding on (a) the fluid dynamics of filtration, and (b) the node-fibril microstructure of the membrane.

1 Introduction

Membrane filters are used in a wide variety of applications. A large filtration membrane area is often desirable in order to filter large volumes quickly; but users would prefer to keep the filter unit of compact size. One way to meet these potentially conflicting aims is to pleat the filter and pack it into a cylindrical cartridge housing, as indicated in Figure 1. Before pleating, the membrane is typically sandwiched between porous support and drain layers, which are pleated along with the membrane filter. Such cartridge filters are very widely used, but it has long been known in the industry that these pleated filter configurations underperform relative to the equivalent-area flat membrane filter [1–4]. This report briefly examines two possible reasons for this: (a) the very different fluid dynamics in the two configurations; and (b) possible changes to the node-fibril microstructure (see Figure 2) of the membrane caused by the pleating process itself.

We first discuss some possible approaches to solving the fluid dynamics through a porous layer sandwich of complex shape, and present some flow patterns that were computed for configurations approximating a pleated filter. We then propose a simplified model for particle capture within an idealized pleated membrane and present preliminary results showing how the particle capture differs between the pleated and flat configurations. Finally, we briefly discuss some considerations that may be relevant for the internal membrane microstructure at the folds, and present some estimates for how membrane performance might be impacted at these locations.

*Contact Author: Department of Mathematical Sciences, New Jersey Institute of Technology, Newark NJ 07102-1982

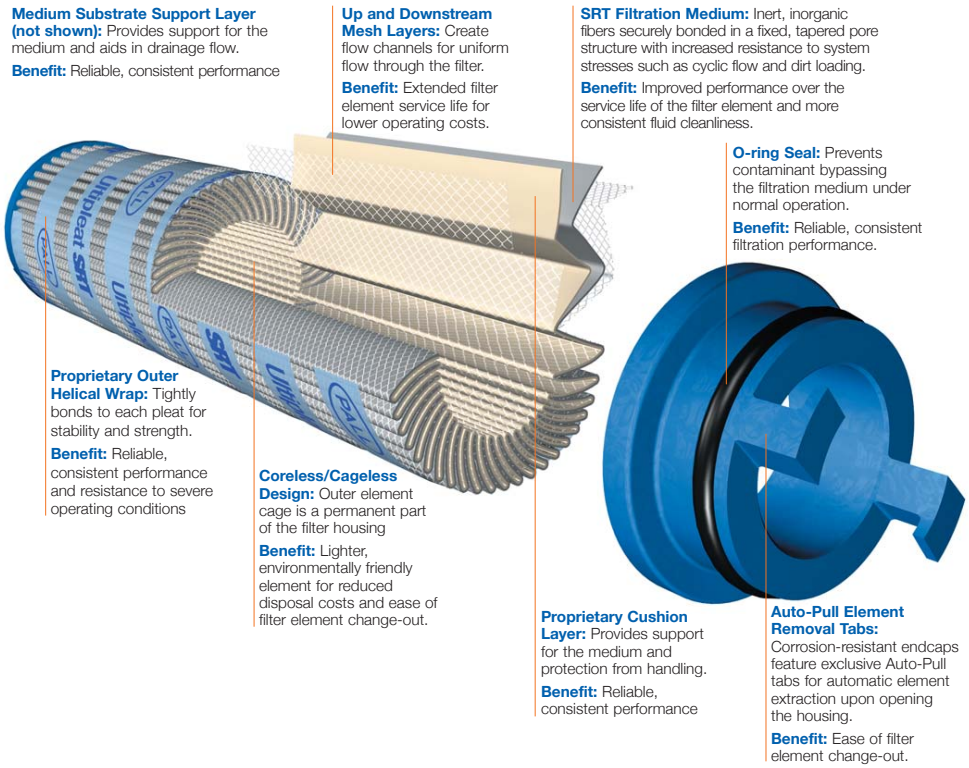

Figure 1: Typical geometry of a pleated membrane filter cartridge (taken from Pall's Power Generation catalog, available at http://www.pall.com/pdfs/Power-Generation/PowerGeneration_Catalog.pdf).

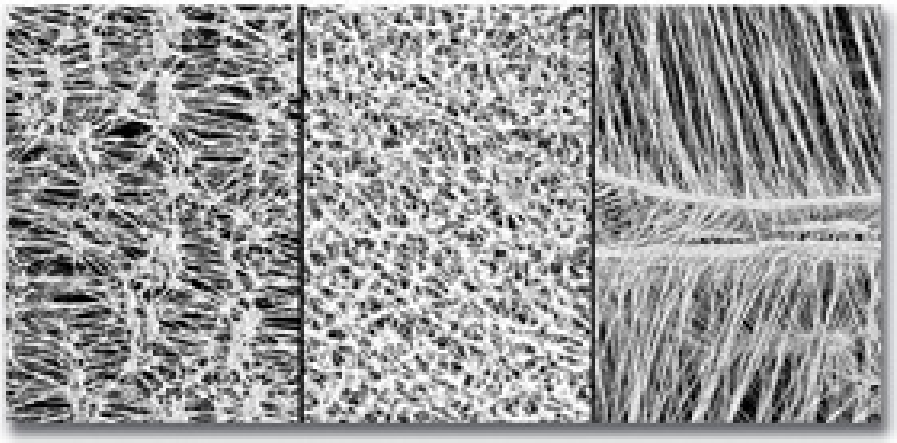

Figure 2: Examples of different types of node-fibril microstructure within a membrane filter (taken from www.gore.com/en_xx/products/filtration/micro/microfiltration_media.html).

2 Fluid dynamics of the pleated membrane

Before considering any details of particle capture we first look at some idealized flows through sections of pleated membranes to see how this differs from the uniform flow that would be observed through the equivalent flat membrane. In this section, we present results of numerical simulations of steady fluid flow through a pleated sandwich structure comprising three layers of porous media representing the support, the membrane, and the drain layer. In each layer, we assume uniform and isotropic permeability. For simplicity, we assume equal permeabilities (k_1) for the support and drain layers on either side of the membrane filter, and a much smaller value for the filter membrane permeability (k_2). The averaged Darcy pore pressure (fluid velocity potential) satisfies an elliptic PDE (below) which we solve using Finite Element Analysis (FEA). All numerical results are obtained using `FEniCS` [5]. The following table summarizes model parameters after nondimensionalization: lengths are scaled with the total thickness of the membrane plus support and drain layer sandwich (h_1, h_3 denote dimensionless support/drain layer thicknesses upstream, downstream, respectively, while h_2 is the dimensionless membrane thickness); pressures are scaled with the total pressure drop. In the following subsections, we consider different scenarios.

Table 1: Non-dimensionalised model parameters for numerical simulation of steady fluid flow through a pleated sandwich structure comprising three layers of porous media.

description	symbol	numerical value
thickness of the sandwich	$w = h_1 + h_2 + h_3$	1.0
inner curvature radius of root and tip	r	1.0
length of straight segment	$2l$	4 or 40.0
membrane thickness	h_2	0.25
mid-line of membrane	$h_1 + h_2/2$	0.6
relative permeability of the membrane	$k_m = k_2/k_1$	0.0001 to 0.5

2.1 Loosely-pleated membrane: Uniform pressure on support/drain surfaces

As an idealized geometry for a section of a periodically loosely-pleated region, we consider a computational domain containing two annular sectors connected by a rectangle (figure 3). The triangular mesh contains 128 elements per unit length, giving an approximate mesh size of 0.008. Darcy flow is assumed within each layer of the sandwich. Permeability changes discontinuously between the membrane and the support/drain layers, which we approximate with a continuous permeability function $k(x, y)$ that varies rapidly across the boundary between the layers. We therefore solve

$$\nabla \cdot (k \nabla p) = 0$$

within all 3 layers, with $p = 1$ on the left-hand layer boundary and $p = 0$ on the right-hand layer boundary driving flow through the sandwich (these constant pressure boundary conditions restrict this analysis to a loosely-pleated scenario where no significant pressure gradients develop along the length of a fold).

Figure 3 shows the setup, and a preliminary numerical solution of the problem. Figure 3(a) shows the chosen permeability map, in which the membrane permeability is set to 0.01 while the support/drain permeability is 100, four orders of magnitude larger (a reasonably typical permeability ratio). Since the permeability is so much lower in the membrane filter the pressure drop occurs almost entirely across this layer (Figure 3(b)). Variation in the fluid velocity is clearly visible around the curved boundaries within the support/drain layers: high velocities appear at the inner side of the tip and the outer side of the root; low velocities appear at the outer side of the tip and the inner side of the root. However, due to the much smaller permeability the fluid velocity within the membrane filter itself shows almost no spatial variation between the straight portion and the curved ends. This suggests that, as far as the membrane filter is concerned, flow variations due to the pleating may not be significant.

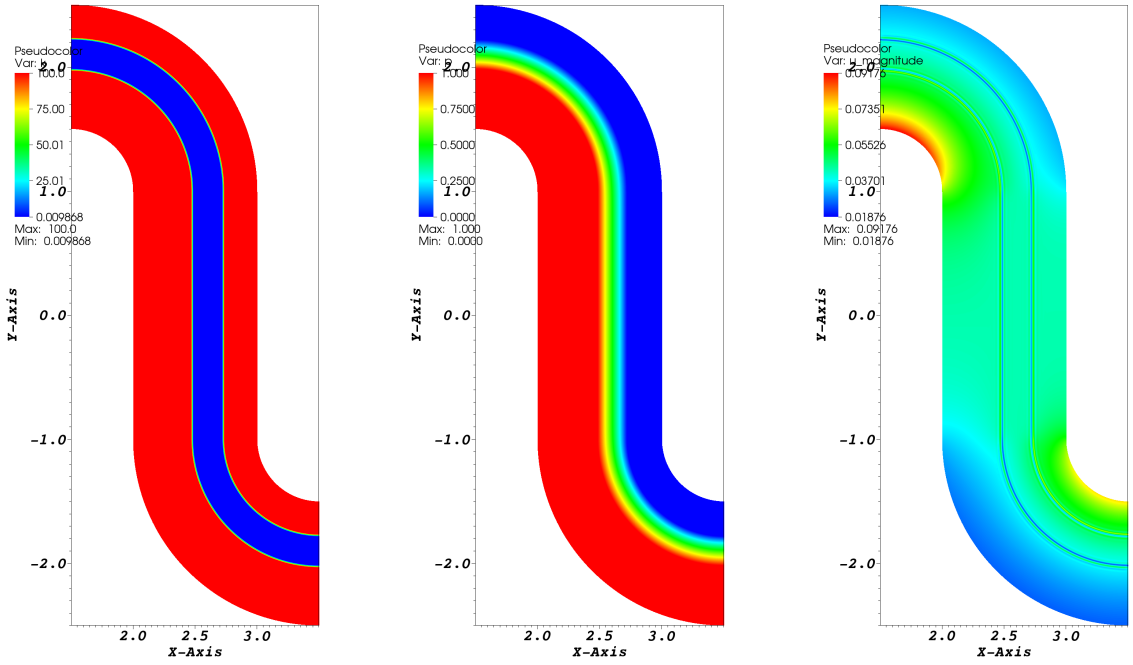

(a) permeability $k(x, y)$ (b) pressure $p(x, y)$ (c) magnitude of fluid velocity $|\boldsymbol{j}(x, y)|$

Figure 3: Steady fluid flow through a sandwich structure comprising three layers of porous media. (a) The permeability of the membrane is assumed to be four orders of magnitude lower than for the adjacent support and drain layers, as described in the text. (b) The largest pressure drop is found across the membrane; pressure is relatively uniform across the much more permeable support/drain layers. Note the constant pressure $p = 1$ and 0 applied at the bottom and top boundaries, respectively. (c) Magnitude of the fluid velocity.

2.2 Tightly-packed pleats: Folded membrane embedded in porous rectangular box

The previous idealized geometry could be appropriate to a loosely-folded pleat with large gaps between adjacent support layers, that might be approximated by the uniform pressure boundary conditions assumed there. To model a more tightly packed array of pleats we now consider a thin curved membrane embedded in a rectangular domain of a porous medium. The geometry is similar to that of Figure 3(a) except that the red regions expand to cover all white areas, and to make the geometry more realistic, we increase the length of the straight membrane segment from 4 to 40 dimensionless units. Instead of applying a pressure difference on the curved surface of the pleated structure we now prescribe a unit pressure drop across the lower and upper rectangle boundaries, and periodic conditions across the left- and right-hand rectangle boundaries. The lower/upper rectangle boundaries represent the outer/inner cylindrical surfaces of the pleated filter schematized in Figure 1. The membrane permeability is set to unity in this example, and the support/drain permeability is varied (but is always larger than 1).

Figure 4 shows the spatial profile of the fluid flow through the straight segment of the pleated structure for different permeability ratios between the support and drain structure and the membrane. The y-direction here is as in Figure 3(a): parallel to the straight section of the pleat. The velocity has been normalized with respect to the expected velocity, $\boldsymbol{j} = j_0 \boldsymbol{e}_y$, in a flat sheet ($r \to \infty$), which (a simple 1-d calculation, not included here, reveals) depends on the permeability of the membrane (k_m) according to $j_0 = (43.25 + 0.25/k_m)^{-1}$. Note that the curves are not symmetric about $y = 0$ due to the membrane's off-center position. With smaller permeability ratios, fluid flow across the membrane concentrates around tip and root of the pleat, as indicated by decreased contributions from the straight segment (a). At high enough permeability ratios the flow profile through the membrane is approximately parabolic (b) (in this case the simplifying assumption of linear pressure profile, $p(y)$, along the boundaries of the straight segment of the membrane, is valid). For a membrane permeability sufficiently small compared to that of the support and drain layers (which we anticipate in practice), flow within the membrane parallel to the straight segment (the y-direction) is negligible (c).

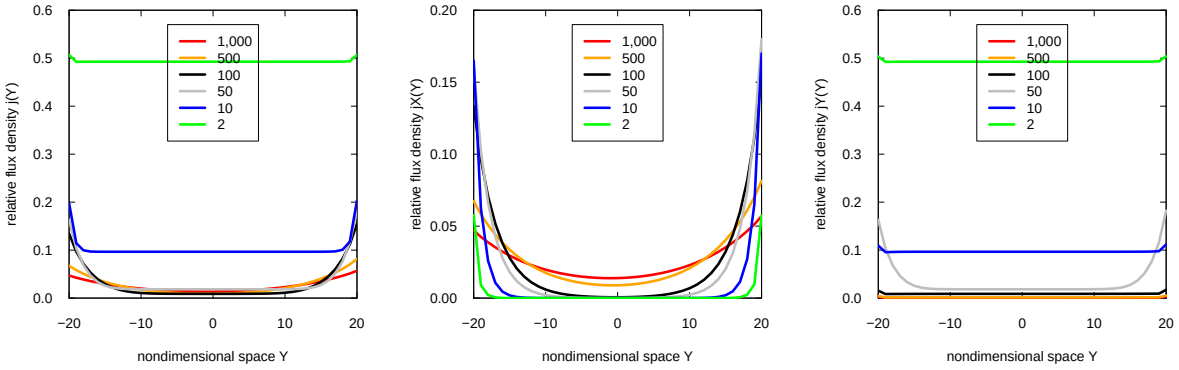

(a) $|\boldsymbol{j}|/j_0$ (b) component j_x/j_0 (c) component j_y/j_0

Figure 4: Velocity profiles along the straight segment of a pleated membrane. (a) Relative magnitude of the velocity. (b,c) Components of the fluid velocity in x- and y-direction, respectively. Colours code for relative permittivity, k_m^{-1}.

2.3 Results and Outlook

In these subsections §§2.1, 2.2, we have analyzed steady Darcy flow of an incompressible fluid through a sandwich structure comprising three layers of porous media. Qualitatively different flow fields were observed for cases of loose and tight packing of pleats. Quantitative analysis of the influence of the permeability of

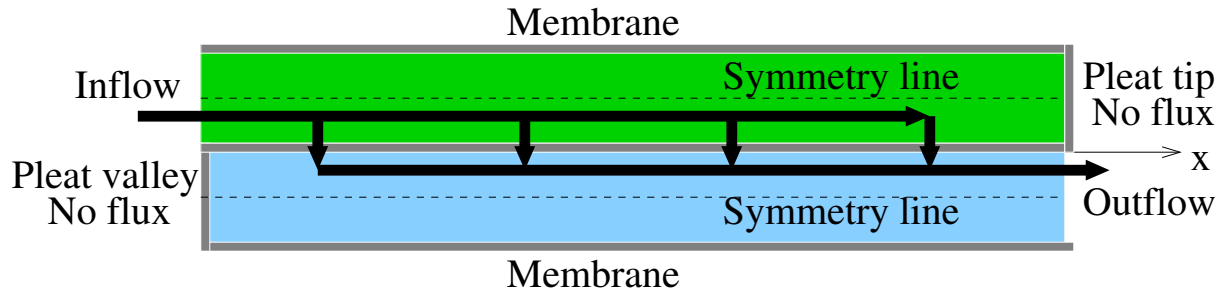

Figure 5: Idealized pleat geometry showing problem setup for the particle-trapping problem.

the membrane showed under which circumstances a parabolic flow profile appears in the straight segment of the pleat. The code developed for these simulations can be easily adapted to alternative geometries, for example altering the tip and root curvatures or the position of the membrane within the sandwich structure. In the case of tight pleat packing and high permeability ratio, which we expect in practice, the proportion of flux passing through the pleated ends is very small relative to the total flux through the straight segment, which motivates the approximate particle-trapping model proposed below.

3 Simple model for particle capture in an idealized pleat

Motivated by the above observation that only a small proportion of fluid flows through the folded ends of the pleated membrane (taking no account of possible membrane degradation at these folds; see §4 below) we now consider membrane function in terms of particle capture using a highly simplified model geometry in which the curvature of the folded ends is neglected. We restrict attention to the more relevant case of tightly-packed pleats, and consider a folded section of membrane represented by a rectangular sandwich as sketched in Figure 5, where filtrate flows in from the left through the upper porous slab (support/drain layer), is forced through the membrane, and then flows out on the right through the lower porous slab. The filtrate carries particles, which can be trapped by the membrane. Each support/drain layer has Darcy flow through it, and we model the membrane separating them as a simple permeable layer, length S in the x-direction (the length of a single pleat). We monitor the membrane's permeability as a function of the number of open (unblocked) pores per unit area, N, which we assume to be a decreasing function of the local flux per unit area, Q:

$$\frac{\partial N}{\partial t} \propto -Q$$

(the proportionality constant here must be estimated from experimental data). Initially, $N(x,0) = N_0$ (constant), the total number of pores per unit area of a clean membrane. When a pore is blocked by a particle, we assume its resistance increases by a fixed amount, ρ_b. For the exposition here we suppose that pores are cylindrical, of radius a, so that the resistance of an unblocked pore can be written explicitly in terms of the pore permeability $\kappa(a) = \pi a^4/(8\mu)$ and the membrane thickness d. With these assumptions, which might be appropriate for the early stages of membrane clogging (before a "cake" of additional resistance begins to form on the membrane) we have

$$\text{Resistance of unblocked pore:} \quad \frac{d}{\kappa(a)}$$
$$\text{Resistance of blocked pore:} \quad \rho_b + \frac{d}{\kappa(a)}.$$

The total flux per unit area through the membrane is then related to the pressure drop across the membrane by the sum of fluxes through unblocked and blocked pores:

$$Q = \Delta P \left(\frac{N}{d/\kappa(a)} + \frac{N_0 - N}{\rho_b + d/\kappa(a)} \right).$$

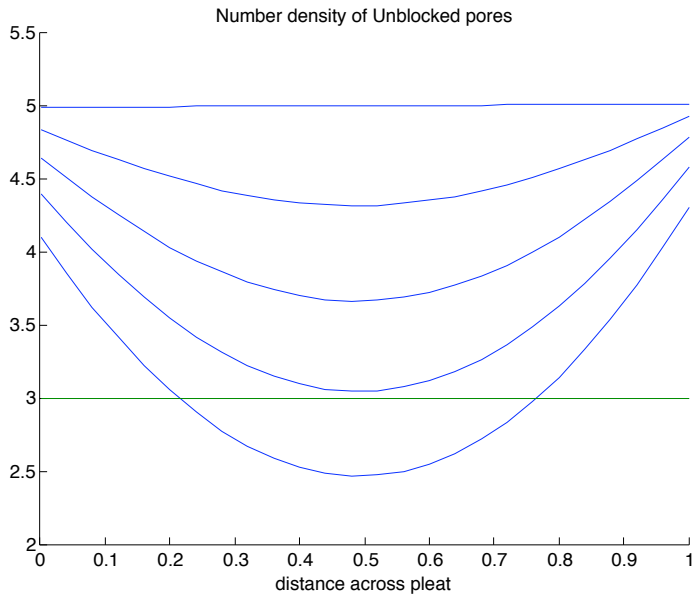

Figure 6: Number density of unblocked pores over time as a function of distance x along the pleat, for the idealized pleat geometry and pore-blocking model described above. Each blue curve represents $N(x,t)$ at a different time, with the curves moving downwards as t increases. The green horizontal line represents the final state for the equivalent flat membrane, and should be compared to the lowest blue curve.

The flat (unpleated) membrane case is especially simple then: N is spatially homogeneous, decreases linearly in time, and the pressure drop across the membrane for a given flux Q can be calculated from the above expression. For our simplified pleat geometry, with the additional assumption that the flow regions are all slender (small aspect ratio) the fluid flow problem in each region may be solved analytically. The pressure drop ΔP then varies spatially, leading to local variations in the flux per unit area, inducing spatial variations in the concentration of blocked pores, $N(x,t)$ (because the local flux through the membrane varies spatially).

The solution procedure over time is as follows: The number of unblocked pores per unit area is initially constant, N_0. The membrane permeability is therefore spatially uniform, and we solve for the fluid flow through the pleat. This yields the spatially-varying pressure drop, $\Delta P(x)$, and hence the spatially-varying flux per unit area, $Q(x)$, satisfying

$$\int_0^S Q(x)\,dx = Q_{\text{tot}}$$

(this assumes that the total flux Q_{tot} through the pleat length $0 \le x \le S$ is specified; if instead the total pressure drop is specified to be constant in time then we enforce this constraint instead). We then time-evolve $N(x,t)$ according to this local membrane flux,

$$\frac{\partial N}{\partial t} \propto -Q(x,t)$$

to find $N(x,t)$ at the next timestep. This determines the new membrane permeability; we solve for the fluid flow through the pleat again; and so on. A Matlab code was written to solve this problem, and a preliminary result is shown in Figure 6 (in the absence of experimental data on constants of proportionality these were chosen arbitrarily). The graph clearly shows how the membrane evolves to be nonuniformly permeable over time (lower values of N correspond to fewer unblocked pores and thus lower permeability: the flow within the pleated structure leads to the membrane blocking primarily near the middle of the pleat, compared to the uniform blocking of a flat membrane. The simulation in Figure 6 is for the situation in which the same flux is enforced for the two cases and thus, since the same total number of particles should be carried per

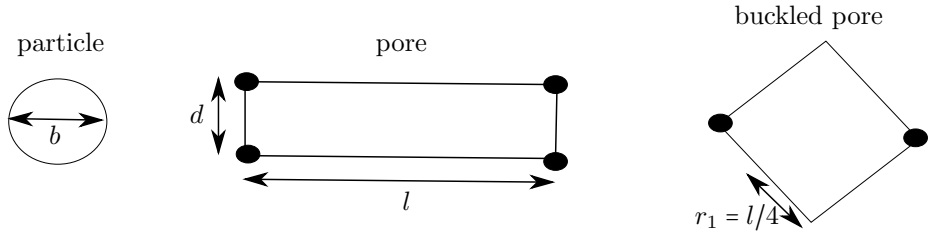

Figure 7: Schematic showing how a typical node-fibril arrangement in an unstressed membrane (center) may buckle under compression (right) to a pore configuration that allows a typical particle (left) to pass through.

unit time for these simulations, the net particle capture in the two cases is almost identical. We would however expect differences between the two cases for the case in which pressure drop, rather than total flux, is enforced.

4 Degradation of the filter via bending

We conclude our report with a brief consideration of how mechanical effects may compromise the membrane's interior node-fibril structure under folding.

4.1 Mechanical considerations

When folded into pleats, the filter membrane will either be under tension or compression at the bends, depending on the asymmetry of the support and drain layers on either side. This tension/compression could cause changes to the microstructure of the filter, and hence lead to changes in permeability. Tension is unlikely to cause sufficient expansion to the short axis of the pores to affect the permeability. Under compression, however, the fibrils may buckle, opening larger pores through which particles may now pass. Therefore we focus on changes in pore size when the membrane is under compression.

The maximum compressive strain the filter will experience (when it lies on the inner boundary of the bend) will be approximately 1/10, for typical dimensions of membrane and support/drain layer thicknesses. If we suppose that this strain is due to some proportion B of the pores buckling maximally (i.e. allowing the largest possible particle to pass through; in some sense a 'worst case' scenario), we can estimate B by considering the compressive strain in a linear array composed of unbuckled and buckled pores (center and right-hand subfigures in Fig 7). For 10% total strain we have, with l is the length of the average long fibril,

$$\frac{Bl/\sqrt{2} + (1-B)l}{l} \approx 0.9 \quad \Rightarrow \quad B \approx 0.34,$$

so that approximately 1 in 3 pores can open to this maximal size. This gives a number density of large pores of $N_1 = \frac{1}{3ld}$, where d is the length of the average short fibril (see Fig.7). The half side length of the large pores created will be approximately $r_1 = l/4$ (Fig.7, right-most figure). This estimate is for a single individual layer of fibrils, therefore we need to calculate the probability that such large pores may line up to form open channels through the system through which a particle may travel.

If we place another layer with the same number density of equivalently sized larger holes (independently distributed) on top of this layer, the number density of holes created which are large enough for a particle to pass through both layers will be $N_2 = (2(r_1 + r_1 - b))^2/(3ld)$ where b is the diameter of the particle, and

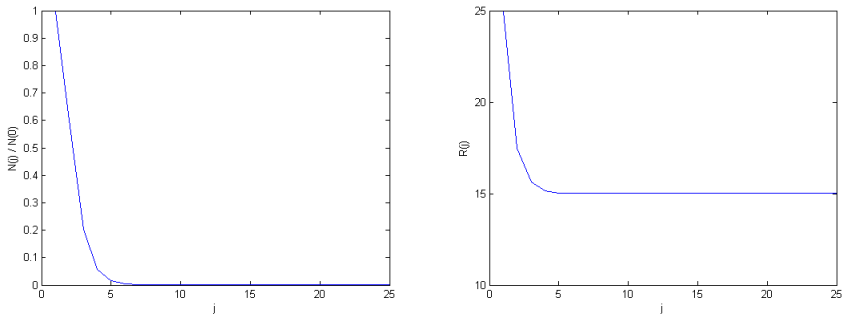

Figure 8: The typical number density of large open pores and their average size vs number of layers.

the average half side length of the large pores created will be $r_2 = \frac{1}{4}(r_1 + r_1 + b)$.[1] Hence the composite filter consisting of $m+1$ such individual layers has $N_{m+1} = \frac{(r_1+r_m-b)^2}{3r_1 d} N_m$, $r_{m+1} = \frac{r_1+r_m+b}{4}$. As the number of layers increases, the number density of open channels becomes vanishingly small (Fig. 8). Given that we anticipate thousands of layers of fibrils in a typical membrane filter, these estimates suggest that the filter performance will not be adversely affected by being under compression. We note, however, that a key assumption made was that the "large pore" distribution due to the buckling is independent from one layer to the next. Given that fibrils also connect adjacent layers (the structure is more like a 3d network than isolated layers), this assumption is quite likely incorrect, and the "large pore" distributions of adjacent layers may well show significant correlation. A more sophisticated analysis would be needed to model and account for such correlations.

5 Summary

This report has considered three key sub-problems that are important for the performance of pleated membrane filters: (i) fluid dynamics through a curved membrane surrounded by support/drain layers; (ii) particle capture and subsequent membrane blocking in a pleated membrane (compared with the equivalent flat unconfined membrane); and the membrane structure degradation that may result from the folding of a membrane with node-fibril microstructure. Our results, while preliminary, suggest that the fluid dynamics, which is very different in a pleated geometry when compared with that through a simple flat membrane, is key to the difference in performance noted. In particular, we note significant spatial variation in the membrane blocking between the two cases, even when the same total flux is enforced; and we would expect to see yet more pronounced differences in performance under conditions of equivalent total pressure drop.

Over the course of the workshop the group considered several other approaches to the fluid dynamical problem. This report contains only those we believe to be most relevant to the problem at hand. Other approaches considered include a study of flow through a flat membrane sandwich with a variable pressure distribution on both external surfaces, intended to mimic the nonuniform pressure distribution within a pleated sandwich. Details of other work carried out are available on request. An exact approach based on conformal mapping was also considered; this is included in the Appendix.

[1] Note that this argument assumes that the large pores are at least as large as a particle but may be considerably larger – thus holes in adjacent layers do not need to be perfectly aligned in order for particles to pass through the double layer. However, the requirement that the large holes have a minimum size equal to the particle size means that the particle size appears in our estimates.

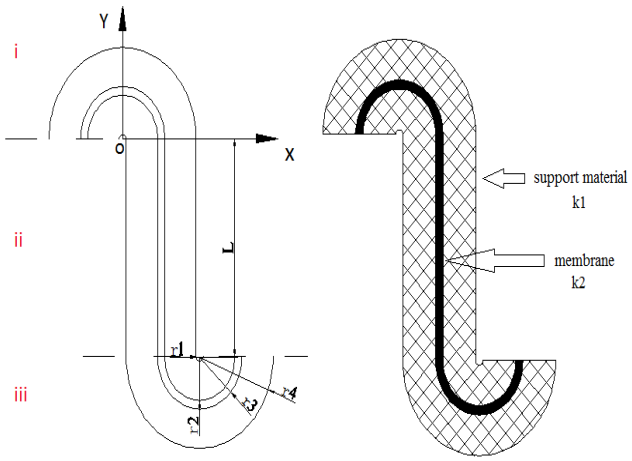

Figure 9: Geometry for the conformal mapping approach.

A Conformal Mapping Approach

We consider the problem of finding the Darcy flow through an 'S'-like domain representing one complete pleat consisting of two bends. As mentioned in the introduction, the domain is composed of a central porous filter membrane, surrounded by two support/drain porous layers, and is schematized in Figure 9.

The pressure within the porous medium satisfies Darcy's law, which for an incompressible fluid yields

$$\nabla \cdot (k \nabla p) = 0.$$

where k is the permeability (piecewise constant in our problem). With the geometry of Fig.9 the equation is difficult to solve, but since p satisfies the Laplace equation on each sub-domain we can use conformal mapping (under which Laplace's equation is invariant) to transform the boundary value problem onto a simpler domain.

We break the domain into three sections, the top semi-circle, the lower semi-circle, and the middle rectangle connecting the semi-circles, and apply a conformal mapping to each semi-circular sub-domain. We calculate the pressure in the new mapped domains, then map back to the original domains. Lastly, we match the solutions between the three sub-domains using the continuity of both pressure and its normal derivative.

The first conformal mapping takes the top semi-circular annulus to a rectangle in the first quadrant (see Fig.10):

$$f(z) = \ln(z) \qquad \text{for } z \in \mathbb{C}$$

The second mapping is similar, but combined with a translation of the semi-circle to the origin (Fig.11):

$$\tilde{z} = g(z) = z - r_4 - r_1 + iL, \quad f(\tilde{z}) = \ln\left(\frac{1}{\tilde{z}}\right).$$

With these mappings, we can easily solve for the pressure. We can do this when the boundary pressures P_0 and P_1 are constant. Using the solution in the 1-dimensional flow problem, we know the pressure in this rectangular domain is $p = A_i u + B_i$ where A_i and B_i are constants, but differ in each layer, $i = 1, 2, 3$, and must be determined. Substituting for $u = \ln(\sqrt{x^2 + y^2})$ maps the solution back to our original domain. The pressure mapped back to the original domain becomes:

$$p = A_i u + B_i = A_i \ln(\sqrt{x^2 + y^2}) + B_i$$

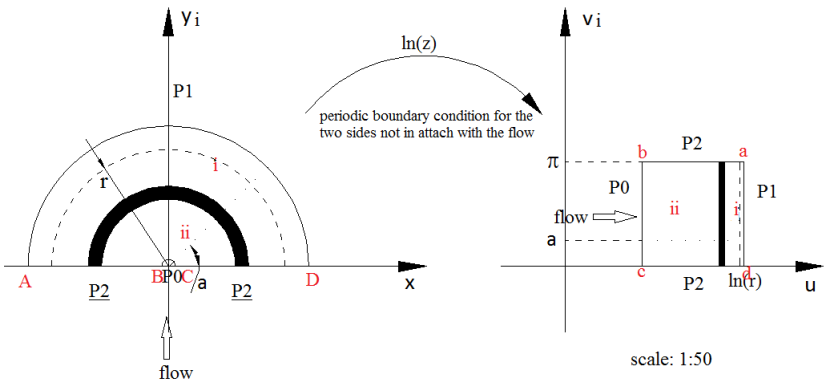

Figure 10: Conformal mapping of the top semicircle to a rectangle.

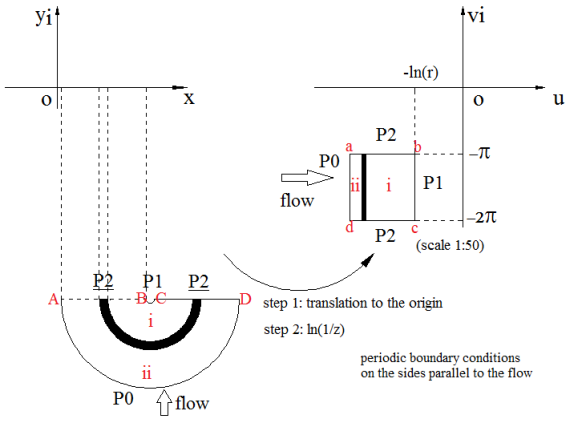

Figure 11: Conformal mapping of the lower semicircle to a rectangle.

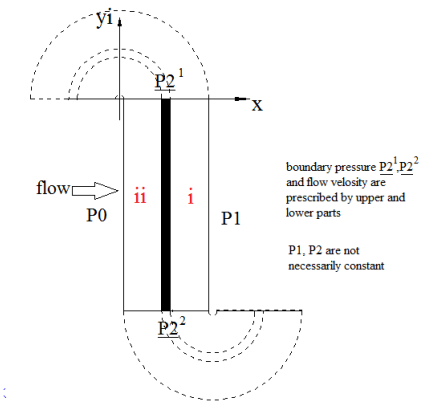

Figure 12: The problem on the central rectangular domain.

To find the pressure on the boundary, we set $y = 0$ (similarly, we can find the normal derivative along the boundary). Analogous methods give the pressure in the lower semicircular domain.

The middle rectangular domain does not need a conformal mapping: we just have to piece together each of the three sub-domains requiring that the pressures and the normal derivatives match along the two boundaries where the sub-domains meet. Finding the pressure through the central domain subject to these matching conditions requires a numerical approach, which we have not yet completed.

With the conformal maps for the separate domains found, his method has the advantage that it can be easily generalized to the case when the boundary pressures P_0 and P_1 are more complex (for example, arising from the solution to some exterior flow problem). It can be applied to many scenarios, making it a good method to find the pressure within each of the three layers.

References

[1] Brown, A.I. An ultra scale-down approach to the rapid evaluation of pleated membrane cartridge filter performance. *D.E. Thesis, University College London* (2011).

[2] Brown, A.I. Scale-down prediction of industrial scale pleated membrane cartridge performance. *Biotech. Bioeng.* **108** (4), 830-838 (2011).

[3] Brown, A.I., Levison, P., Titchener-Hooker, N.J., Lye, G.J. Membrane pleating effects in 0.2μm rated microfiltration cartridges. *J. Membrane Sci.* **341**, 76-83 (2009).

[4] Giglia, S., Rautio, K., Kazan, G., Backes, K., Blanchard, M. Improving the accuracy of scaling from discs to cartridges for dead end microfiltration of biological fluids. *J. Membrane Sci.* **365**, 347-355 (2010).

[5] Logg, A., Mardal, K.-A., Wells, G. N. *et al.* Automated Solution of Differential Equations by the Finite Element Method, dx.doi.org/10.1007/978-3-642-23099-8, (2012), Springer.